

THE EXTRACTION SYSTEM FOR THE SUPERCONDUCTING CYCLOTRON AT THE UNIVERSITY OF MILAN

E. Fabrici and A. Salomone

University of Milan and Istituto Nazionale di Fisica Nucleare  
via Celoria 16, 20133 Milano, Italy

**Abstract.** - The extraction solution planned for the Milan superconducting cyclotron is presented together with a survey of beam dynamics prior to extraction.

**1. Introduction.** - This paper presents the extraction scheme planned for the Milan superconducting cyclotron. It is the result of an extensive analysis of beam dynamics prior to extraction and of the extracted beam optics carried out for a set of representative ions spanning the entire operating range of the machine both in terms of charge to mass ratio and magnetic field level.

The main machine characteristics are extensively reported in ref. 1. We recall only that the Milan cyclotron is a three sectors-three dee machine with a pole radius of 90 cm. The  $K_b$  is 800 and the  $K_{foc}$  200.

The extraction system employs two electrostatic deflectors followed by a set of magnetic channels made of saturated iron bars. The excitation of the  $\nu_r = 1$  resonance provides the necessary beam to beam separation at the entrance of the first electrostatic deflector. Consequently the amplitude and the phase of the 1st harmonic field bump necessary to excite the resonance have been carefully investigated.

The present results are obtained with field maps calculated up to  $R=114.3$  cm, thus allowing the trajectory integration only up to  $R=111-112$  cm. Field maps extending up to  $R=200$  cm, to be used for both injection and extraction purposes, are now in preparation. So far, they are fully consistent with the solution presented here.

**2. Beam dynamics prior to extraction.** - The starting conditions chosen for the acceleration runs are the radial and axial eigenellipses on the equilibrium orbit at an energy corresponding to several turns, typically 20 or 30, before the  $\nu_r = 1$  resonance. Accelerated orbits are tracked on  $360^\circ$  maps to take into account the field produced by the hardware needed for extraction. As stated above, seven magnetic channels are used. They produce a sizable 1st harmonic, which is compensated by inserting three additional iron bars.

Fig.1 presents a schematic view of the median plane of the machine showing the hills and valley contours together with the extraction system. The electrostatic deflectors are labelled E, the magnetic channels M and the compensating bars C.

The two bars C1A and C1B compensate for the field 1st harmonic due to M1 and M2. Two bars are required because a coil support link (see fig.6 of ref.1 for all the details of the median plane geometry) will prevent the insertion of a single bar exactly at  $180^\circ$  from M1 and M2. The bar C2 compensates for the overall 1st harmonic field due to channels from M3 to M7.

The field produced by the magnetic channels and the compensating bars are added to the threefold- $120^\circ$  symmetric field map thus giving the  $360^\circ$  map used for the

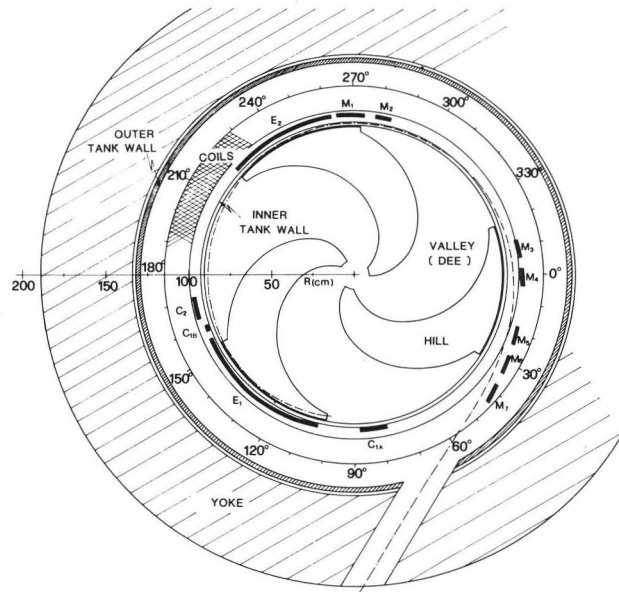


Fig.1 - Median plane sketch showing the extraction system.

beam dynamics calculations. For the case of the ion with a charge to mass ratio,  $Z/A$ , equal to 0.5 and a nominal center field value for which isochronism has been calculated,  $B_0$ , equal to 31.1 kgauss, the fig.2 presents the average field,  $\bar{B}$ , the 1st harmonic,  $C_1$ , the 2nd harmonic,  $C_2$ , produced by the magnetic channels only on the left side and the compensated ones on the right side. The resulting 1st harmonic perturbation is around 1 Gauss inside the machine and less than 1 Gauss in proximity of the  $\nu_r = 1$  resonance.

Table I summarizes the results of the acceleration runs giving, for each of the representative ions investigated, the extraction energy,  $T/A_F$ , the final phase,

$\Phi_F$ , the 1st harmonic amplitude used,  $B_1$ , and its phase,  $\Phi_1$ .

We note that the final phase for the 100 MeV/n case is quite large (54). It has been checked that it is mainly due to the decrease of the average field introduced by the saturated iron bars. In fact as can be seen from the curve labelled  $\bar{B}$  on the right of fig.2, the reduction of the average field is  $\sim 30$  Gauss on the last turn,  $R=87$  cm, and can be as high as 75 Gauss due

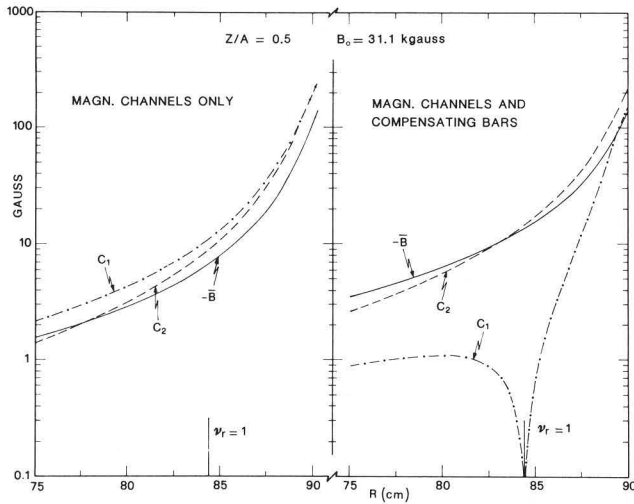


Fig. 2 - Average field, 1st and 2nd harmonics produced by the hardware needed for extraction.

to the 4.4 cm scalloping of the orbits. To improve the final phase of the most relativistic ions the more recent map calculations include the average field due to the magnetic channels and the compensating bars directly in the process of isochronising the field. This method in very recent calculations has allowed to reduce the extracted phase down to  $\Phi_f \sim 40^\circ$ .

Table I - Acceleration data for representative ions.

Z/A	B <sub>0</sub> (kG)	T/A <sub>f</sub> (MeV/n)	Φ <sub>f</sub> (deg)	B <sub>1</sub> (G)	Φ <sub>1</sub> (deg)
.08	49.5	5.62	13	-	-
.24	46.6	47.98	17	2.5	240
.3	41.6	61.14	34	1.	300
.5	31.1	100.36	54	1.5	0
.5	22.	44.92	17	5.	270
.3	22.	15.24	10	-	-
.08	25.	1.37	28	-	-

The phase space behaviour at extraction has been analysed at  $\vartheta = 100^\circ$ , azimuth which is very close to the entrance of the 1st deflector as apparent from fig.1. Fig.3 presents the radial phase space plots obtained for the Z/A=.5 ions with B<sub>0</sub>=22 kgauss (T/A 45 MeV/n) and B<sub>0</sub>=31.1 kgauss (T/A 100 MeV/n). For both beams the ellipses are drawn only for the extracted turn and the previous one to show the beam to beam separation which is typi-

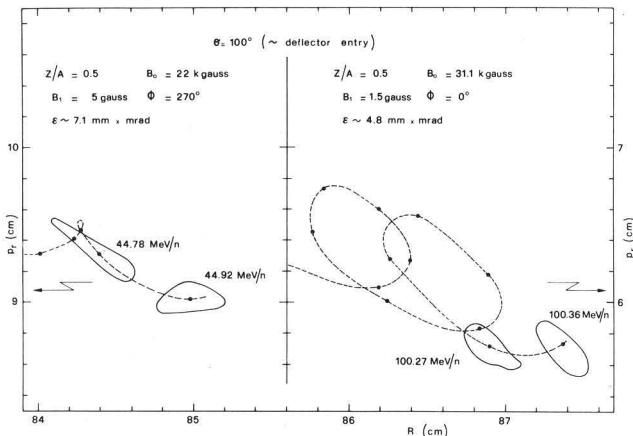


Fig. 3 - Radial phase space plots at extraction for the ions with Z/A=.5 and B<sub>0</sub>=22 and 31.1 kgauss.

cally 1-1.25 mm. A greater beam to beam separation can be achieved for the lower energy beams.

As evident from fig.3 the extraction radius is around 85 cm for the 45 MeV/n ions and it is around 87.4 cm for the 100 MeV/n ions thus requiring a range of radial movement of at least  $\pm 1.2$  cm for the first electrostatic deflector. This range of movement cannot be appreciably reduced since: i) the 100 MeV/n ions cannot be extracted at a more internal radius, since the electric field on the deflectors is realistically limited to 140 kV/cm. ii) the  $\nu_r + 2\nu_z = 3$  resonance is crossed, for the 45 MeV/n ions, at an average radius of only 84.8 cm.

The approaching of the  $\nu_r + 2\nu_z = 3$  resonance can be seen on fig.4 showing the axial phase space of the extracted turn (solid line) and the successive one (dashed line). The increase of the extraction radius of only 0.55 cm produces a doubling of both z and p<sub>z</sub>.

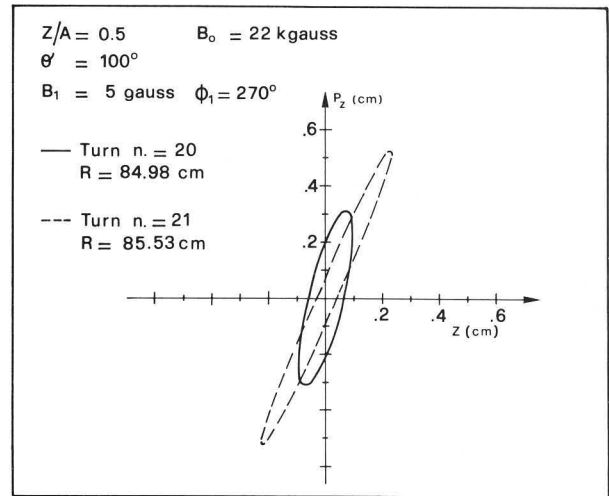


Fig. 4 - Axial phase space at extraction for the ion with Z/A=.5 and B<sub>0</sub>=22 kG (see text for details).

3. Extraction system.- The extraction elements are shown in fig.1 and listed in table II with all the relevant parameters as the initial and final azimuths,  $\vartheta_i$  and  $\vartheta_f$ , the maximum electric field, E<sub>max</sub>, the magnetic field bias, ΔB, the focusing gradient,  $\partial B / \partial x$ , and the required range of radial movement,  $\pm \Delta R$ .

Table II - Extraction element parameters

	ϑ <sub>i</sub> (deg)	ϑ <sub>f</sub> (deg)	E <sub>max</sub> (kV/cm)	ΔB (kG)	∂B/∂x (kG/cm)	± ΔR (mm)
E1	104	156	140	-	-	12
E2	222	262	140	-	-	8
M1	264	274	-	-2.	3.86	3
M2	278	284	-	-1.8	2.12	4
M3	348	354	-	-1.2	3.63	7
M4	358	364	-	-1.2	3.63	7
M5	378	384	-	-1.2	3.63	7
M6	388	394	-	-1.2	3.63	6
M7	398	404	-	-1.2	3.63	6
C1A	78	88	-	-	-	19
C1B	158.85	161	-	-	-	19
C2	164	172	-	-	-	14

The two electrostatic deflectors are positioned in two successive hills, the extracted rays being inside the dee in between. The 1st one is 52° long and the 2nd is 40° long and it is immediately followed by two magnetic

channels the first one  $10^\circ$  long and the second one  $6^\circ$  long. All the other magnetic channels are  $6^\circ$  long and, after M5, regularly spaced by  $4^\circ$ . The large azimuthal clearance between M4 and M5 is required for the insertion of a beam probe.

Fig.5 shows on a Cartesian ( $\vartheta, R$ ) plot the extraction trajectories up to M4 for the ions with the maximum and minimum charge to mass ratio  $Z/A=0.5$  and  $Z/A=0.08$  respectively, both of them at the maximum and minimum energies. From this figure it is evident the range of radial movements required for the electrostatic deflectors. An interesting effect comes from the large orbit scalloping variation which is observed between  $B_0=49.5$  kgauss and  $B_0=22$  kgauss. It turns out that a "rigid" deflector, with only two actuators, cannot accommodate all the extraction trajectories. Therefore it is necessary to split each deflector in two parts with a joint approximately in the middle of each deflector<sup>1)</sup>. In this way it will be possible to center the deflectors along all the extracted trajectories with an accuracy of  $\pm 0.5$  mm.

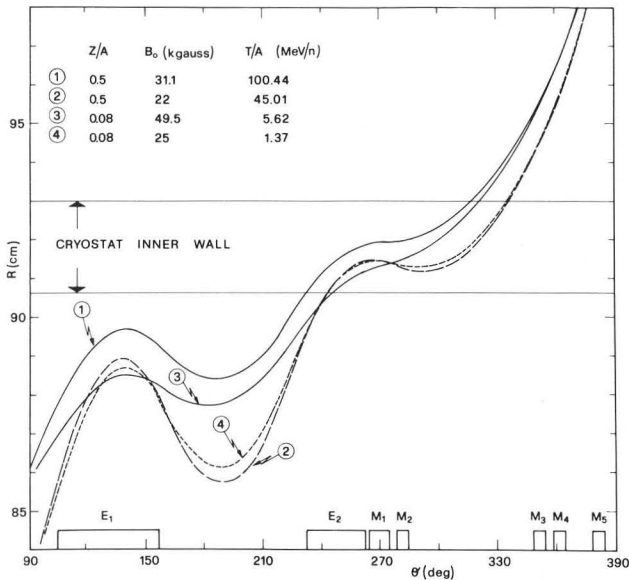


Fig.5 - Extraction trajectories of four representative ions on a Cartesian ( $\vartheta, R$ ) plot.

At this stage, a geometry similar to the MSU<sup>2)</sup> one has been adopted for the magnetic channels and the compensating bars. The latter and M1 are supposed to be mounted from the inside of the machine as the electrostatic deflectors. All the other magnetic channels will be mounted from the outside to allow an easy removal of some of them for the extraction of ions with  $B_0$  low as 22 or 25 kgauss where the full set would be radially overfocusing.

The beams envelopes look well confined along all the extraction path both in the radial and axial dimensions, as can be seen in fig.6 for the case of the ion with  $Z/A=0.5$  and  $B_0=22$  kgauss. The radial and axial phase spaces obtained at  $\vartheta=412^\circ, R \sim 111$  cm, near the exit from the cryostat, are presented in fig.7 for the same set of ions whose trajectories are plotted in fig.5.

4. Conclusions.- The extraction system looks so far fully capable of meeting the design requirements. More calculations are in progress to study the beam behaviour during the yoke traversal. In this region an active channel (may be superconducting) will be adopted.

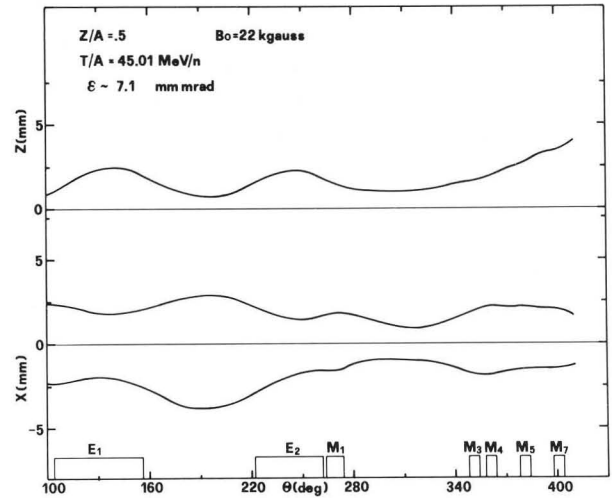


Fig.6 - Radial and axial beam envelopes along the extraction path for the ion with  $Z/A=0.5$  and  $B_0=22$  kgauss.

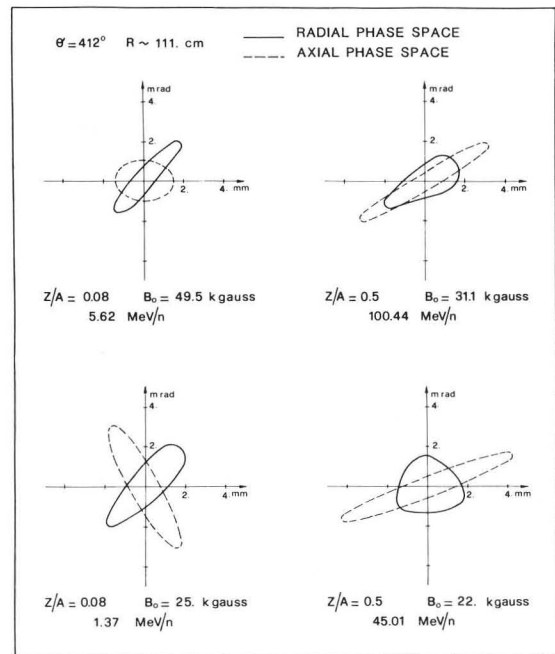


Fig.7 - Radial and axial phase spaces near the exit from the cryostat ( $\vartheta=412^\circ, R \sim 111$  cm) for four representative ions.

Another possibility is a combination of active plus passive. This will be decided in the coming months. Tests on a prototype deflector being built will establish the feasibility of the elements as presently conceived.

#### References

1. E. ACERBI et al., The Milan Superconducting Cyclotron Project, paper presented to this Conference.
2. E. FABRICI, D. JOHNSON and F.G. REMINI, Nuclear Instruments and Methods, **180** (1981) 319.